GEOMAGNETISM AND AERONOMY, English Translation, VOL. 35, NO. 2, OCTOBER 1995
Russian Edition: MARCH–APRIL 1995

Temperature variations in the high-latitude thermosphere during a substorm

Yu. N. Koren'kov, F. S. Bessarab, and V. V. Klimenko

Kaliningrad Observatory of Institute of Terrestrial Magnetism, Ionosphere, and Radio Wave Propagation, Russian Academy of Sciences

Abstract. Numerical simulation results are presented of spatial-temporal variations of the thermospheric temperature and Joule heating during a typical isolated substorm on March 25, 1987, observed by European Incoherent Scatter. It is demonstrated that during the expansion phase of a substorm the neutral gas temperature spatial distribution at the altitudes of the lower and upper thermosphere is governed by the Joule heating source distribution. Maximum temperature values are reached in the upper thermosphere 20 min after the end of the expansion phase of a substorm and in the lower one 30 min after the end. During the recovery phase of a substorm the dynamic processes above 200 km lead to a shift of the temperature maximum into the noon sector, although the maximum of the Joule heating stays in the evening sector. The latter demonstrates that the neutral gas temperature enhancement in the dayside cusp region probably is not directly related to the Joule heating or to the soft electron precipitation during a substorm.

Introduction

The high-latitude thermosphere is the region of the terrestrial atmosphere where during geomagnetic disturbances there happens a principal deposition of the energy, coming from the magnetosphere in a form of energetic precipitating particle fluxes, field-aligned currents, and electric fields of magnetospheric origin. Experimental and theoretical investigations of the processes accompanying the energy dissipation in the high-latitude thermosphere have been carried out by many authors [*Forbes et al.,* 1987; *Fuller-Rowell,* 1984; *Fuller-Rowell and Rees,* 1981, 1984; *Gizler and Troshichev,* 1983; *Goncharov et al.,* 1979; *Kolesnik and Korolev,* 1985; *Millward et al.,* 1993; *Roble et al.,* 1987; *Sharapov and Mishin,* 1987; *Straus et al.,* 1985]. For example, *Gizler and Troshichev* [1983] and *Sharapov and Mishin* [1987] have considered the nature of the Joule source variations during a substorm. The neutral gas dynamics in periods of electric field enhancement at high latitudes has been studied by *Fuller-Rowell* [1984], *Fuller-Rowell and Rees* [1981, 1984], *Forbes et al.* [1987], and *Straus et al.* [1985]. Theoretical studies of the neutral atmospheric composition in disturbed conditions have been conducted by *Kolesnik and Korolev* [1985] and *Goncharov et al.* [1979]. Temporal variations of the thermospheric thermal structure have never been investigated in the above papers jointly with the Joule heating variability during a substorm, calculated in a self-consistent way. The most complete from that point of view was the work by *Millward et al.* [1993], in which the ionospheric parameters and the Joule source have been calculated in a self-consistent way jointly with the thermospheric parameters. However, that paper has been dedicated to a special case of a strong electric field (~ 200 mV m^{-1}) occurrence in a narrow latitude band (70–78°N) of the morning sector. That case represents a unique event, which requires a special consideration and cannot be considered as a typical situation during a substorm.

In this paper investigation results are presented of the temporal variations of the temperature and the Joule heating source in the thermosphere during a typical isolated substorm. The numerical simulation was conducted using the global self-consistent model of the terrestrial thermosphere, ionosphere and protonosphere (GSM TIP). The model has been described in detail by *Namgaladze et al.* [1988, 1990, 1991]. The difference between this study from others conducted earlier is that the present model allows one to calculate in a self-consistent way all the plasma electrical parameters in the high-latitude region of the terrestrial atmosphere, if the field-aligned current system and the precipitating electron flux are given during a substorm.

0016–7932/96/3502–0013$18.00/1

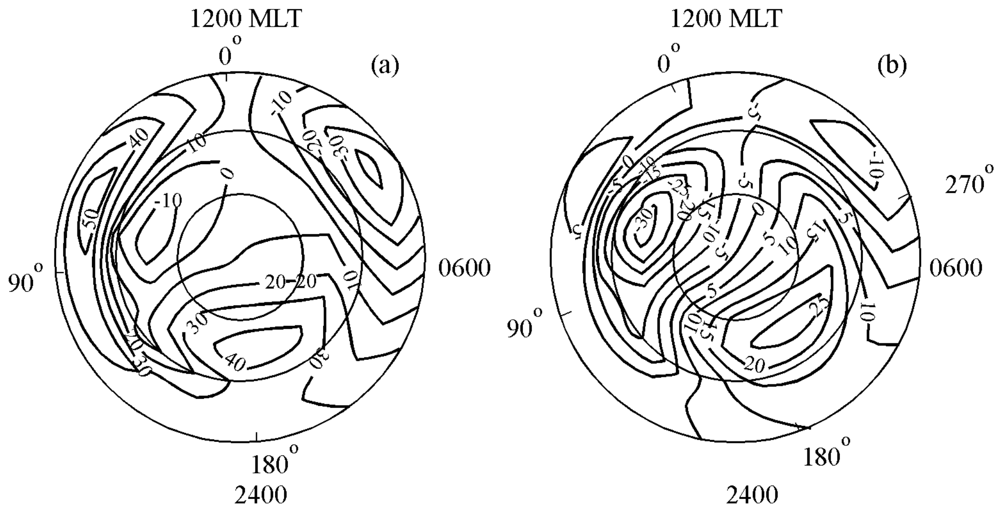

Figure 1. Isolines of the electric field potential for two moments: (a) 1700 and (b) 1800 UT.

Formulation of the Problem

As was mentioned above, a substorm effect modeling in the thermosphere was performed using the global self-consistent model of the thermosphere, ionosphere, and protonosphere. The model was developed in the Kaliningrad Observatory of IZMIRAN and described by *Namgaladze et al.* [1988, 1990, 1991]. Also used was a modification of the above model created at the Polar Geophysical Institute and described by E. V. Barbolina et al. (unpublished manuscript, 1993) and *Namgaladze et al.* [1993]. Not presenting a detailed description of the model we remind readers that its input parameters are the solar UV radiation, the currents in both, the first and the second zones of the high-latitude region, and the fluxes of soft (< 0.5 keV) and hard (> 0.5 keV) electrons, precipitating into the auroral region of the ionosphere.

The output parameters of the model are nonstationary global three-dimensional distributions of the principal components (O_2, N_2, O), concentrations of molecular (O_2^+ + NO^+) and atomic (O^+, H^+) ions and of electrons and their temperatures, the neutral and the ionized particle velocities, and the electric field potential of the dynamo and of magnetospheric origin. All data are presented for the height interval of 80 km up to the geocentric distance of 15 Earth radii.

A substorm on March 25, 1987, was chosen for the study. The ionospheric effects of that substorm were observed at the EISCAT site (70°N, 19.2°E) and were described by *Collis and Hoggstrom* [1989, 1991].

The substorm started at 1540 UT; the fact was fixed by the geomagnetic data of Kiruna station and by a sudden enhancement of the electric field above EISCAT. At 1700 the electric field reached its maximum value of about 60 mV m^{-1} and at 1900 UT returned to its initial value of about 5 mV m^{-1}. The total duration of the substorm was about 3 hours. The electric field enhancement was accompanied by an increase of the precipitating particle flux above EISCAT, which was clearly manifested at 1630 UT by a sudden increase of the electron concentration at 111 km from 2×10^4 cm^{-3} to 1×10^5 cm^{-3} [*Collis and Hoggstrom,* 1991]. Analyzing the results by *Collis and Hoggstrom* [1989, 1991], one is able to conclude that the above isolated substorm had all the principal features of a typical disturbance of that class. From 1540 until 1630 UT the growing phase was observed (a gradual increase of the electric field); from 1630 until 1700 UT the expansion phase was observed (a sharp increase of the electric field and of the precipitating particle fluxes); and from 1700 until 1900 UT the recovery phase was observed.

The substorm was modeled in the following way. The field-aligned currents of the first and the second zones at geomagnetic latitudes 75° and 65°N were increasing during the linear phase from the initial values of 4×10^{-8} and 1.5×10^{-7} A m^{-2} up to the maximum values of 6×10^{-7} A m^{-2} in both zones. At the moment of switching to the expansion phase the current model was accomplished by an introduction of one more field-aligned current region at latitudes 75° and 70° (the so-called substorm current spike) with an amplitude of 10^{-6} A m^{-2}. The above spike was "switched off" during the recovery phase at 1835 UT on the background of the field-aligned current amplitude depletion in the first and the second regions. At 1900 UT the currents corresponded to the initial ones.

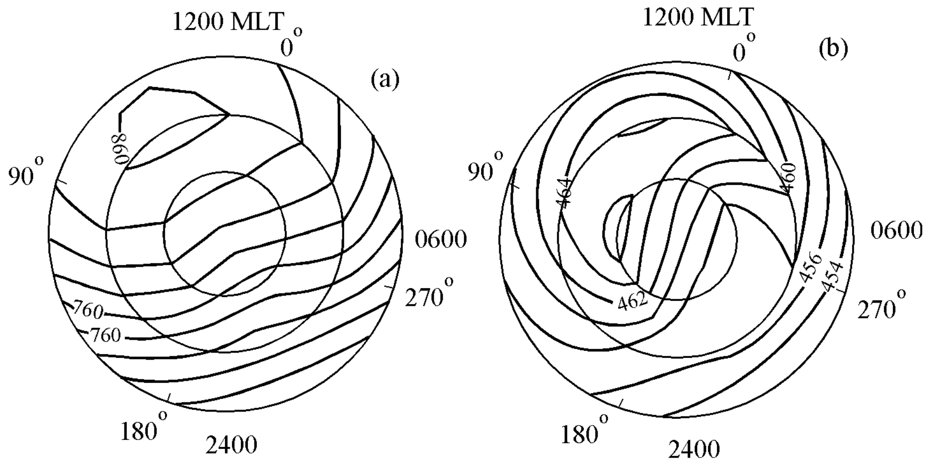

Figure 2. Isolines of the neutral gas temperature at 1540 UT at altitudes of (a) 279 km and (b) 127 km.

The flux of the precipitating electrons with the characteristic energy 3 keV was enhanced from 1630 until 1640 UT in the nighttime sector of the ionosphere by 40 times in comparison to quiet conditions (from 1.0 erg cm^{-2} s^{-1} to 40.0 erg cm^{-2} s^{-1} in the maximum). A crescentlike precipitation zone was shifting during the substorm expansion phase into the morning sector (0300 MLT), and during the recovery phase it was shifting back into the midnight sector (0000 MLT). The temporal variations of these input parameters were chosen to minimize a difference between the calculated and the measured parameters of the electric field and the electron concentration at 111 km above EISCAT. The solar UV-radiation fluxes and the soft electron fluxes were taken in the same way, as in our former calculations [*Namgaladze et al.,* 1991], and were not changed during the whole substorm.

Simulation Results

The results for the northern hemisphere are presented in the polar geomagnetic coordinate system (geomagnetic latitude 60–90°N). The geomagnetic longitudes are indicated at the latitudinal circle 60°.

Figure 1 shows the isolines of the electric field potential for two moments of universal time: 1700 (Figure 1a) and 1800 (Figure 1b). It is apparent that the potential distribution is characterized at the moment of the substorm maximum development by a four-vortex structure. Two vortices are formed by the first zone currents at 75° latitude and two are formed by and the second zone currents at 65° latitude in the morning and the evening sectors. The maximum meridional electric field is observed in the afternoon sector (1700 MLT) between the vortices of region one and region two the first and the second field-aligned current. Such a convection system is due to an approximate equality between currents of the first and the second zones and by the presence of the current spike in the after-midnight sector at that moment of UT.

At 1800 UT (Figure 1b) during the recovery phase the convection system has a structure close to normal with some increase, relative to the quiet level, of the electric potential across the polar cap (55 kV). Figures 2–4 demonstrate the calculation results of the Joule heating and the neutral gas temperature at 127 and 279 km for three moments of time: 1540 UT (Figures 2a and 2b), 1700 UT (Figures 3a and 3b) and 1800 UT (Figures 4a and 4b).

Analyzing Figure 2a one can see that the neutral gas temperature maximum at 279 km is situated in the afternoon sector at a latitude of about 70° and it reaches 860 K. There are two local maxima in the neutral temperature distribution in the lower thermosphere. One maximum is situated in the afternoon sector at latitude 70°, the other maximum is situated in the evening sector at latitude 80°. Let us note that the temperature gradient at the ionospheric $F2$-region heights is directed from the nightside to the dayside, whereas in the lower thermosphere it is directed from the morning sector to the evening sector.

Figures 3a and 3b show isolines of Joule heating (left) and of the neutral gas temperature (right) at altitudes of 279 km (Figure 3a) and 127 km (Figure 3b) at the moment of the expansion phase maximum at 1700 UT.

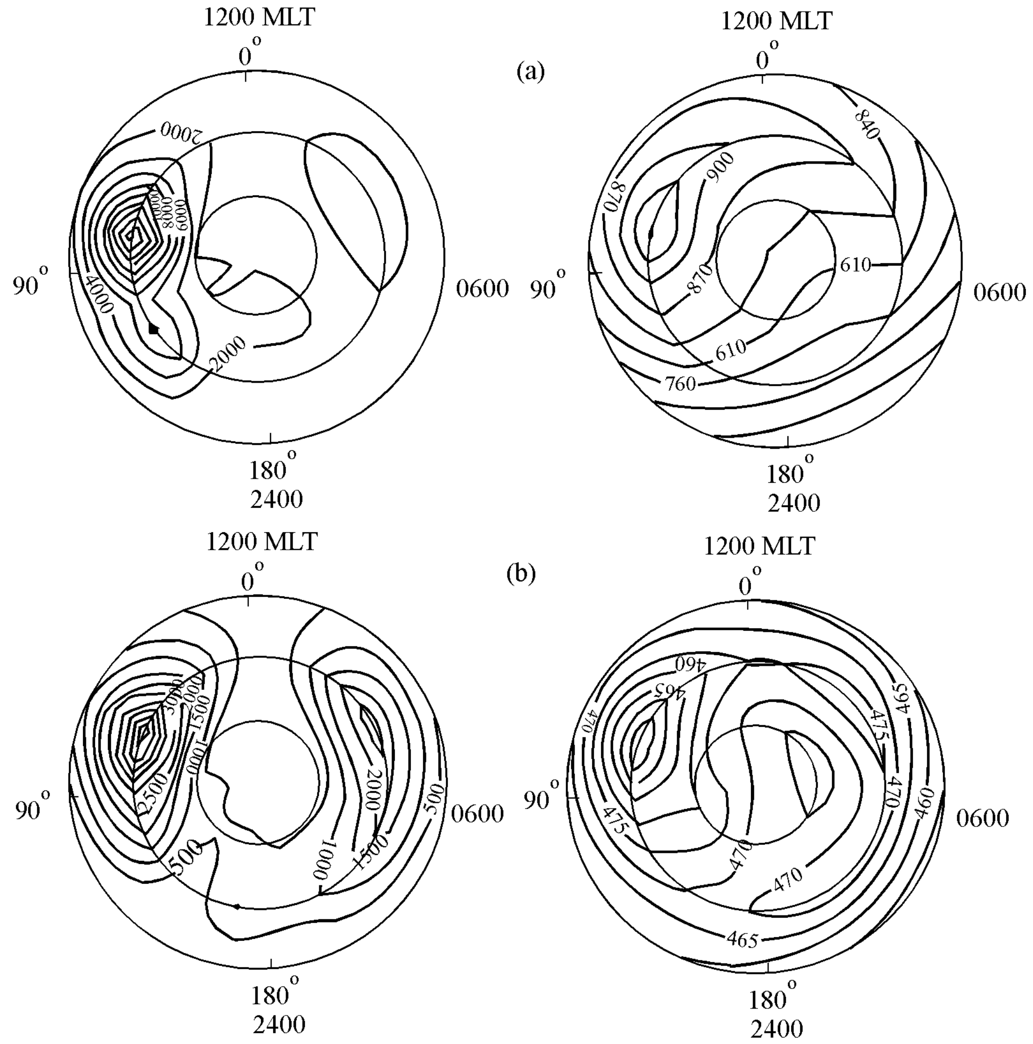

Figure 3. Isolines of the Joule heating rate (K day^{-1}, left) and of the neutral gas temperature (right) at altitudes of (a) 279 km and (b) 127 km at 1700 UT.

It is apparent that at the ionospheric $F2$-region altitudes the maximum of the neutral gas Joule heating is situated in the evening sector (1800 MLT) and is about 20,000 K day^{-1}. There is a second maximum in the morning sector, the value of which is by an order of magnitude lower than the evening maximum. The neutral gas temperature distribution has one maximum corresponding to the evening maximum of the Joule heating.

The Joule heating source in the lower thermosphere has two pronounced maxima in the evening and the morning sectors. The Joule heating value in the evening sector reaches 5500 K day^{-1} and in the morning one – 2500 K day^{-1} in the morning sector. Respectively, there are two maxima in the temperature distribution: the evening (495 K) and the morning (475 K). The temperature gradient is directed across the polar cap in the lower thermosphere along the line 0700–1900 MLT and in the upper thermosphere along the line 0300–1500 MLT.

Figures 4a and 4b demonstrate the isolines of the Joule heating and of the neutral gas temperature at altitudes of 279 (Figure 4a) and 127 km (Figure 4b) during the recovery phase at 1800 UT. It is apparent that there are several maxima in the Joule heating distribution at 279 km. In the evening sector at latitude 70° with a maximum value of 4500 K day^{-1}, in the midnight sector at latitude 80° with a maximum value of 3000 K day^{-1} and in the morning sector (weakly seen) with an amplitude of about 1000 K day^{-1}. The temperature spatial distribution at that altitude (Figure 4a, right) is characterized by one maximum in the afternoon

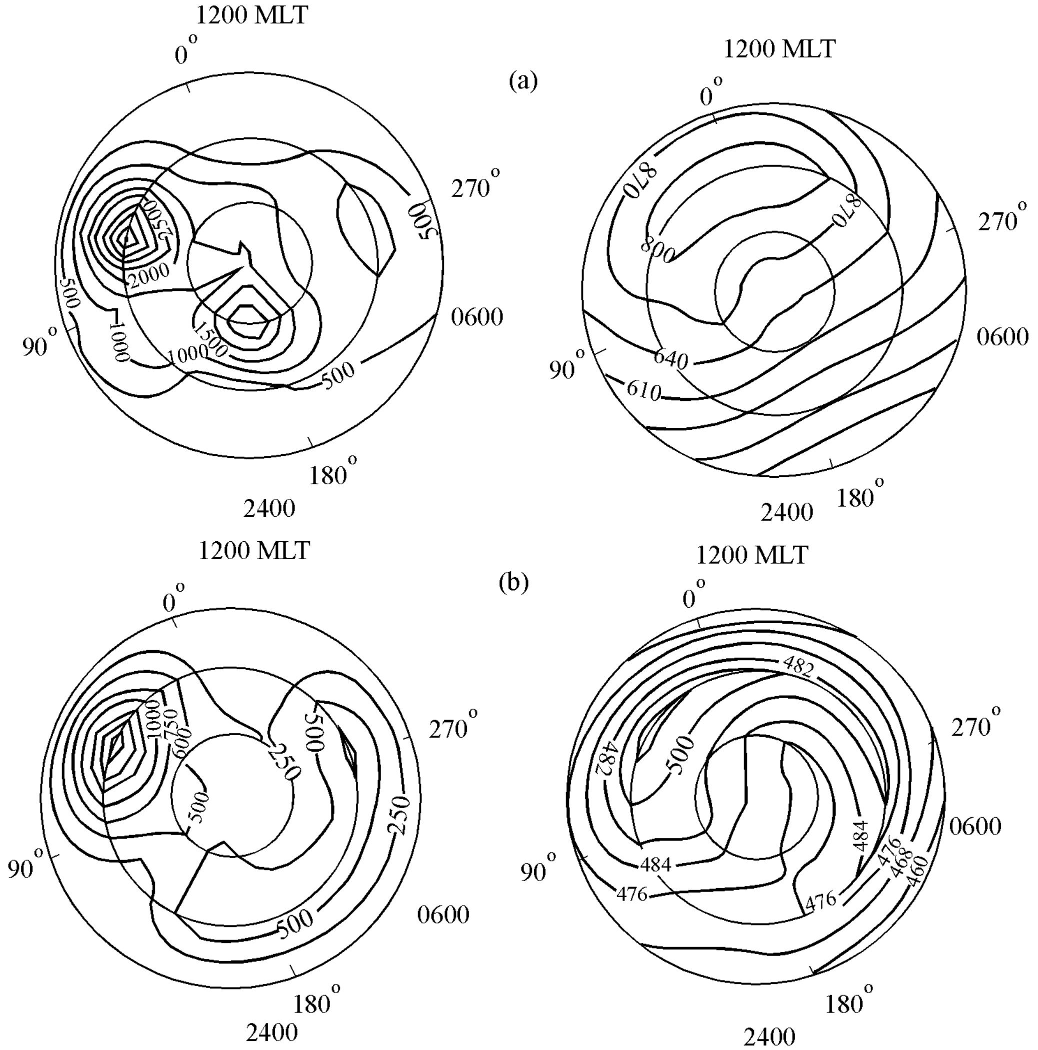

Figure 4. Isolines of the Joule heating rate (K day^{-1}, left) and of the neutral gas temperature (right) at altitudes of (a) 279 km and (b) 127 km at 1800 UT.

sector. Location of that maximum does not coincide with the location of the neutral atmosphere Joule heating maximum.

In the lower thermosphere (Figure 4b) the Joule heating demonstrates a pronounced maximum in the evening sector with an amplitude of 1750 K day^{-1} and the a definite maximum in the morning sector with an amplitude of 750 K day^{-1}. There is a maximum in the temperature distribution at 1500 MLT with an amplitude of 508 K. In the morning sector some increase of the temperature is seen, which may be considered a continuation of the evening maximum. The position of the neutral gas temperature evening maximum nearly coincides with the position of the Joule heating maximum. Let us note that the maximum value of the temperature in the lower thermosphere at 1800 UT is higher than at 1700 UT, whereas in the upper thermosphere the relation is opposite.

Discussion of Simulation Results

The presented results of the numerical simulation demonstrate that the Joule heating distribution in the upper thermosphere at 1700 UT practically has only one evening maximum (Figure 3a), whereas in the lower thermosphere there are two localized maxima (Figure 3b). The ratio of the Joule heating maximum values in the evening and morning sectors is equal to 2, which is related to the spatial distribution of both the electric field and the charged particle concentrations. The main maximum of the molecular ion production at 127 km

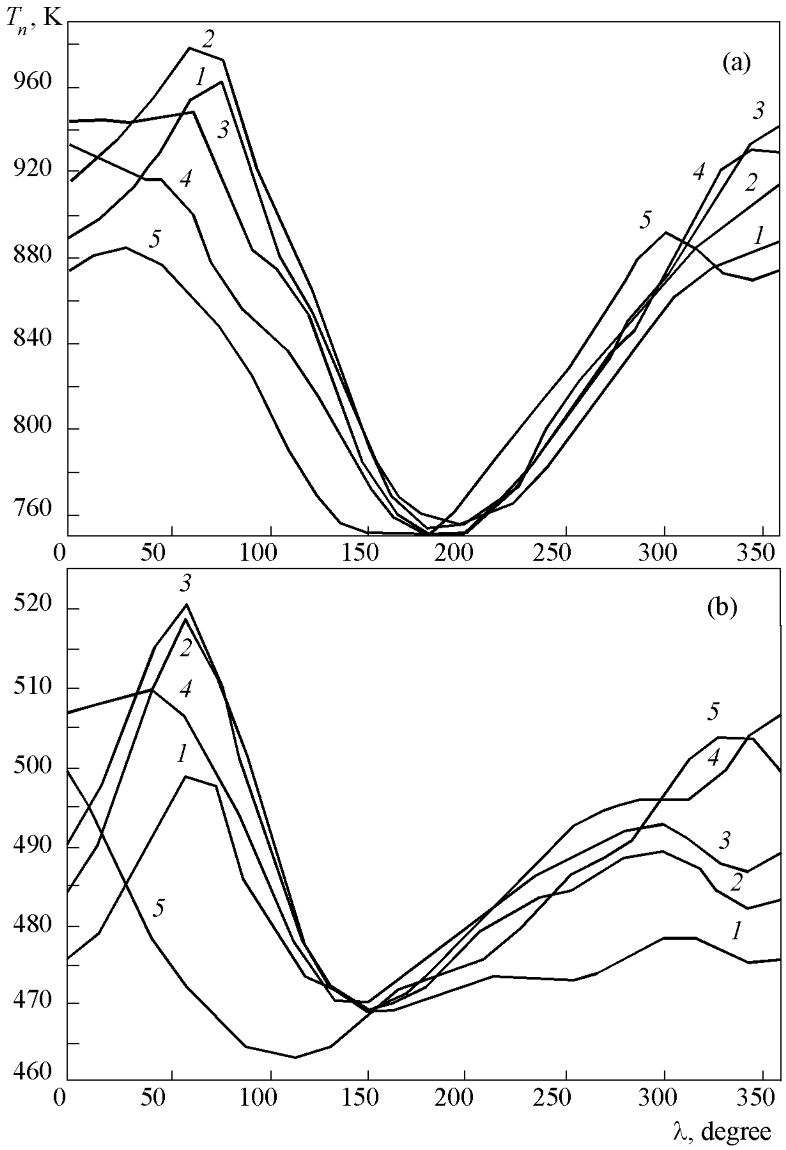

Figure 5. The neutral gas temperature at the geomagnetic latitude 70° versus the geomagnetic longitude at altitudes of (a) 279 km and (b) 127 km at various moments of universal time: 1, 1700; 2, 1720; 3, 1745; 4, 1800; and 5, 1900 (Figure 5a); and 1, 1700; 2, 1720; 3, 1730; 4, 1800; 5, 1900 (Figure 5b).

is situated in the after-midnight sector. As a result, the concentration of the molecular ions in the morning sector is several times higher than in the evening one. Thus in spite of lower values of the electric field strength in the morning sector than in the evening section, the Joule heating rate in the morning sector is comparable with that in the evening sector. At the $F2$-region heights the distribution of the atomic oxygen ions participating in a generation of the Joule heating is nearly the same in the morning and in the evening sectors, but the electric field strength in the evening sector is about 3 times higher then in the morning sector. The latter fact leads to a situation where the evening values of the Joule heating significantly exceed the morning values.

The high Joule heating rates in the evening sector of the upper thermosphere lead to a rapid heating of the neutral gas. It is clearly demonstrated in Figures 5a and 5b, which present a falling off along geomagnetic longitude of the neutral gas temperature distribution at 279 km (Figure 5a) and 127 km (Figure 5b) at the latitude of 70° for various moments of UT. It is apparent that T_n at 279 km at 1700 UT reaches nearly maximum value about 900 K at 75° longitude (the evening sector). This exceeds the background value by about

100 K. T_n is increases 20 K more during the following 20 min, although the electric field is already beginning to decrease.

It is worth mentioning that a rapid enhancement of the electric field initiates a wavelike dynamic process, which is manifested in a different way in the lower and the upper thermosphere. That fact has been mentioned by *Fuller-Rowell and Rees* [1981] in the aspect of the IGW generation and propagation. The above process signature can be found in the performed calculations. For example, the temperature at 279 km in the maximum Joule heating region starts to decrease after 1730 UT, and at longitude 0° it continues to increase, producing a shift of the neutral temperature maximum close to the noon sector. At the latter longitude the absolute maximum is reached around 1700 UT. At 1900 UT (Figure 5a) the maximum is observed already in the prenoon sector. A direct analysis of all the heating sources performed by the method described by *Bessarab and Koren'kov* [1993], has demonstrated that formation of the increased neutral temperature regions in the noon sector of the upper atmosphere at 1800 UT is due to the processes of the convective heat transport and of the adiabatic compression/expansion. A presence of dynamic processes is also apparent, if one compares the spatial distributions of T_n and of the Joule heating source at 1800 UT (Figure 4a). The comparison shows that the Joule heating maximum does not any more determine the temperature maximum position.

The absolute maximum of the neutral gas temperature in the lower thermosphere (Figure 5b) is reached 10 min later (1730 UT) than at the $F2$-region heights. The temperature in the morning sector reach its maximum even later (1800 UT). The temperature increase is smoother. During the following period the temperature in the maximum Joule heating region begins to decrease and in the afternoon sector continues to increase, which indicates a redistribution of the energy due to dynamic processes. However, at 1800 UT the absolute temperature maximum is still related to the Joule heating spatial distribution. At 1900, when the electric field is reduced to its initial value, the general T_n distribution along 70° latitude has one maximum in the afternoon sector, as was the case before the substorm beginning. In those quiet conditions the Joule heating source at the ionospheric $F2$-region heights is, as has been demonstrated by *Koren'kov et al.* [1993], to a significant degree governed by the neutral gas circulation and does not coincide with locations of the electric field maximum values. It is impossible to compare the simulation results with experimental data in a complete way because the snapshot observations of the thermospheric parameter distributions during a substorm are not available.

The most complete data for the substorm on March 22, 1979, which happened under geophysical conditions, closest to the ones studied in this paper, have been obtained in the scope of a special campaign CDAW6. *Sharapov and Mishin* [1987], *Baker et al.* [1985], and *Kamide and Baumjohann* [1985] have published spatial distributions of the electric field potential and of the Joule heating source at various phases of the substorm. Based on that data one can conclude that the Joule heating distribution during the substorm was characterized by a significant temporal variability and by the presence of local spatial maxima in the evening and the morning sectors, as well as in the noon sector. All those facts agree quantitatively with the results of the above described calculations.

The results of numerical simulations of the thermospheric parameters for the conditions of the substorm on March 22, 1979, have been presented by *Roble et al.* [1987]. However, the magnetospheric convection system accepted in the above paper did not correspond to the electric potential spatial picture created by an inversion of the magnetometer measurements on March 22, 1979, and published by *Barber et al.* [1985] and *Kamide and Baumjohann* [1985]. Moreover, spatial distributions of the Joule heating were not presented by *Roble et al.* [1987]; thus a comparison was possible only for the temperature fields. The differences between our calculations and the results of *Roble et al.* [1987] are due, in our opinion, to differences in the adopted electric field potential spatial distribution. General analysis of the results by *Roble et al.* [1987] in an indirect way confirms the above-performed calculations.

Conclusions

Based on numerical simulation results of the spatial distribution of the Joule heating source and of the neutral temperature at various heights one can conclude the following.

1. During the expansion phase of a substorm, which is characterized by the maximum values of the electrical field, the neutral gas temperature spatial distribution at altitudes of the lower and upper thermosphere is determined by the Joule heating spatial distribution. The absolute temperature maximum in the upper thermosphere is reached 20 min after the end of the expansion phase and in the lower thermosphere it is reached 30 min after the end. The above maxima are localized near the maxima of the Joule heating at the corresponding altitudes.

2. During the recovery phase dynamic processes at the $F2$-region heights lead to a shift of the temperature maximum into the noon sector, although the Joule heating maximum is still located in the evening sector. The temperature distribution in the lower thermosphere is

still governed by the Joule heating source. The temperature maximum in the morning sector is reached 45 min later than the electric field maximum, and in the noon sector it is reached 1 hour later.

A direct analysis of the dynamic source distribution indicate its dominating role in the thermospheric thermal balance during the recovery phase of a substorm. Thus the observed temperature enhancement in the noon sector of the upper thermosphere, i.e., in the region of the dayside cusp, probably, is not directly related to the Joule heating.

References

Baker, D. N., et al., The role of heavy ionospheric ions in the localization of substorm disturbances on March 22, 1979: CDAW6, *J. Geophys. Res., 90*, A2, 1273–1281, 1985.

Bessarab, F. S., and Yu. N. Koren'kov, Dynamic process influence on the thermal regime of the upper thermosphere, *Geomagn. Aeron., 33*, 5, 120–126, 1993.

Collis, P. N., and I. Hoggstrom, High resolution measurements of the main ionosphere trough using EISCAT, *Adv. Space Res., 9*, 5, 45–48, 1989.

Collis, P. N., and I. Hoggstrom, High-latitude ionospheric response to a geomagnetic sudden commencement, *J. Atmos. Terr. Phys., 53*, 11/12, 1113–1124, 1991.

Forbes, J. M., R. G. Roble, and F. A. Marcos, Thermospheric dynamics during the March 22, 1979, magnetic storm, 2, Comparisons of model predictions with observations, *J. Geophys. Res., 92*, 6, 6069–6081, 1987.

Fuller-Rowell, T. J., A two-dimensional, high-resolution nested-grid model of the thermosphere, 1, Neutral response to an electric field "Spike," *J. Geophys. Res., 89*, 5, 2971–2990, 1984.

Fuller-Rowell, T. J., and D. Rees, A three-dimensional, time-dependent simulation of the global dynamic response of the thermosphere to a geomagnetic substorm, *J. Atmos. Terr. Phys., 43*, 7, 701–721, 1981.

Fuller-Rowell, T. J., and D. Rees, Interpretation of anticipated long-lived vortex in the lower thermosphere following simulation of an isolated substorm, *Planet. Space Sci., 32*, 1, 69–85, 1984.

Gizler, V. A., and O. A. Troshichev, Heating of the polar ionosphere by the electric currents at various stages of a substorm, *Geomagn. Aeron., 23*, 2, 247–252, 1983.

Goncharov, E. E., et al., On energy sources during a magnetospheric substorm and on their influence on charged and neutral particles distribution in the upper atmosphere, *Phys. Solaritter.*, no. 10, 81–92, 1979.

Kamide, Y., and W. Baumjohann, Estimation of electric fields and currents from international magnetospheric study magnetometer data for the CDAW6 intervals: Implications for substorm dynamics, *J. Geophys. Res., 90*, A2, 1305–1317, 1985.

Kolesnik, A. G., and S. S. Korolev, Thermosphere reaction to the electric field of a magnetospheric origin, in *Modelirovanie Fiziko-Khimicheskikh Protsessov v Polyarnoy Ionosfere*, p. 39, Apatity, 1985.

Koren'kov, Yu. N., F. S. Bessarab, V. M. Smertin, and V. V. Klimenko, A model analysis of the spatial structure of the Joule heating source in the terrestrial thermosphere, *Geomagn. Aeron., 33*(5), 127–134, 1993.

Millward, G. H., et al., Modeling study of the coupled ionospheric and thermospheric response to an enhanced high-latitude electric field event, *Planet. Space Sci., 41*, 1, 45–55, 1993.

Namgaladze, A. A., et al., Global model of the thermosphere-ionosphere-protonosphere system, *Pure Appl. Geophys., 127*, 2/3, 219–254, 1988.

Namgaladze, A. A., et al., Global numerical model of the thermosphere, ionosphere, and protonosphere of the Earth, *Geomagn. Aeron., 30*, 4, 612–619, 1990.

Namgaladze, A. A., et al., Numerical modeling of the thermosphere-ionosphere-protonosphere system, *J. Atmos. Terr. Phys., 53*, 11/12, 1113–1124, 1991.

Namgaladze, A. N., O. V. Martynenko, V. V. Kachala, and E. V. Barbolina, A realization of the global model of the thermosphere, ionosphere, and protonosphere on a personal computer, in *Tez. Dokl. 3 Soveshchania "Matematicheskie Modeli Blizhnego Kosmosa,"* pp. 82–83, Moscow, 1993.

Roble, R. G., J. M. Forbes, and F. A. Marcos, Thermospheric dynamics during the March 22, 1979, magnetic storm, 1, Model simulations, *J. Geophys. Res., 92*, 6, 6045–6058, 1987.

Sharapov, D. Sh., and V. M. Mishin, Joule heating in the high-latitude ionosphere, *Issled. po Geomagn., Aeron. Fizike Solntsa*, no. 79, 98–105, 1987.

Straus, J. M., R. L. Walterscheid, and K. E. Taylor, The response of the high-latitude thermosphere to geomagnetic substorms, *Adv. Space Res., 5*, 4, 289–292, 1985.

(Received April 24, 1994.)